

DIRECTIONAL DUAL-BAND SLOT ANTENNA WITH DUAL-BANDGAP HIGH-IMPEDANCE-SURFACE REFLECTOR

X. L. Bao, G. Ruvio, and M. J. Ammann

Centre for Telecommunications Value-chain Research (CTVR)
School of Electronic & Communications Engineering
Dublin Institute of Technology
Kevin Street, Dublin 8, Ireland

Abstract—A compact dual-band high-impedance-surface EBG structure is employed as a reflector for a dual-band annular-slot antenna. The reflector comprises an array of miniaturized EBG cells which utilizes square patches augmented by four S-shaped corrugated arms to reduce the resonant frequency of the proposed EBG structure. In order to broaden the bandwidth and adjust the frequency ratio for the dual-band EBG structure, a log-periodic spacing between the S-shaped strips is introduced. The combination of microstrip-fed annular slot and EBG reflector provides directional properties for both frequency bands with reduced size and low-profile.

1. INTRODUCTION

Microstrip slot antennas have found application in a wide variety of areas, such as wireless communication systems, RFID, satellite communications and GPS systems [1–5] due to the advantages of low-profile, broad bandwidth and easy fabrication. The drawbacks of slot antennas include bidirectional radiation pattern and low gain. In order to achieve directional radiation characteristics, a slot antenna needs to be combined with a reflector. Generally, the separation between a slot antenna and a conventional metallic reflector is approximately a quarter of a free space wavelength, with different working frequencies requiring different separations in order to achieve best directional properties. However, for dual-band slot antennas it is difficult to realize

Corresponding author: M. J. Ammann (max.ammann@dit.ie).

well matched directional characteristics over both working frequencies when using a conventional metallic reflector.

Techniques have been used to provide directional radiation patterns, such as using the metal cavity reflector [6–8]. Directional radiation patterns have been implemented using Electromagnetic Bandgap (EBG) structures [9, 10], but these investigations only consider a single operating frequency.

In recent decades, there has been a remarkable growth in interest in EBG antennas structures applied to microwave circuits and antennas. A novel EBG structure was employed in microwave filters to suppress passband ripple [11]. In [12], an EBG structure was applied to a low-profile spiral antenna to improve the front-to-back ratio and increase gain. Generally, the period of an EBG structure is about a half-wavelength with respect to the centre-frequency and the bandgap is narrow. So, investigations on compact, broadband and multiband EBG structures have excited many researchers. In [13–15], high-impedance surface (HIS) structures, comprising square conducting patches connected by via to the groundplane, were proposed and analyzed. This realizes a distributed network of inductive and capacitive elements by means of the grounding vias and the proximity of adjacent patches. Other techniques to increase inductance or capacitance have been used to improve characteristics of EBG structures. In [16–18], the convoluted metal strips of EBG cells are employed to increase inductance and reduce the resonant frequency. But the bandgaps are very narrow and only the characteristics of a single bandgap are investigated. Hence, these are not appropriate for dualband antennas.

In this paper, a miniaturized EBG structure, which can provide a dual bandgap is investigated. By adjusting the separation between the strips according to a log-periodic function, the frequency ratio of two bandgaps can be adjusted. Moreover, by using this compact dualband EBG structure as a reflector, the antenna can be smaller, lower profile and improve the gain for both frequencies.

2. THE COMPACT DUALBAND EBG STRUCTURE

An EBG structure can be considered as an LC network model. Its first resonant frequency is given by $f_0 = \frac{1}{2\pi\sqrt{L\cdot C}}$ and the bandwidth of the EBG structure is proportional to $\sqrt{\frac{L}{C}}$. For a HIS cell with square-patch shaped conductor, the values of inductance L and capacitance

C can be approximated by the formula [4]:

$$C = \frac{\varepsilon_0(1 + \varepsilon_r)Pw}{\pi} \cosh^{-1} \left(\frac{Pa}{g} \right), \quad L = \mu_0 \cdot h \cdot (\ln(1/\alpha) + \alpha - 1). \quad (1)$$

where α is the ratio of the via cross sectional area to the EBG unit cell area and h is the thickness of substrate. The period is given by $Pa = g + Pw$, where g is the separation between the patch cells and Pw is the dimension of a cell square conductor. The conducting arms are connected to a small square metal patch, which is connected by via to the groundplane, as shown in Figure 1. These are used to decrease the resonant frequency and reduce the size of the EBG structure. In order to adjust the frequency ratio of the centre frequencies and increase the bandgap of the EBG structure, log periodic elements are employed in the proposed structure. The log periodic structure is shown in Figure 2. The log-periodic ratio is given by:

$$p = \frac{L1}{L2} = \frac{L2}{L3} = \frac{L3}{L4} = \frac{L4}{L5} = \dots = \frac{Ln}{Ln-1} \quad (2)$$

The dispersive curves for the proposed EBG structure were determined using CST MWS. In this case, the proposed compact EBG structure was fabricated on FR4 substrate, which has a relative permittivity of 4.2, a thickness of 1.52 mm and a loss tangent of 0.02. The metal patches are connected to the ground plane using a metal via post of radius 0.5 mm. A multiple parametric sweep was carried out on the log-periodic ratio p and the width w of the strips while the other parameters were kept constant. The results of this numerical analysis led to the following set of parameters and correspond to the largest bandgaps: $p = 1.5$ mm, $w = 0.8$ mm, $Pa = 18$ mm, $Pw = 16.8$ mm, $g = 1.2$ mm, $Sg = 0.4$ mm, $Sa = 2.0$ mm. As seen in the dispersion diagram of Figure 3, two wide bandgaps are realized. The first bandgap is centred at 2.534 GHz (1.596 GHz to 3.491 GHz) and the second bandgap is centred at 4.507 GHz (4.060 GHz to 4.954 GHz).

3. GEOMETRIC ARRANGEMENT FOR ANTENNA WITH EBG REFLECTOR

An annular slot antenna fed by microstrip line can provide dual-band characteristics exciting various modes by adjustment of slot width and the length of microstripline. In this case, a dual-frequency slot antenna is designed, which has mainly bidirectional radiation patterns for both frequency bands. The annular slot antenna geometry is shown in Figure 4 which is also fabricated on FR4. The parameters of the

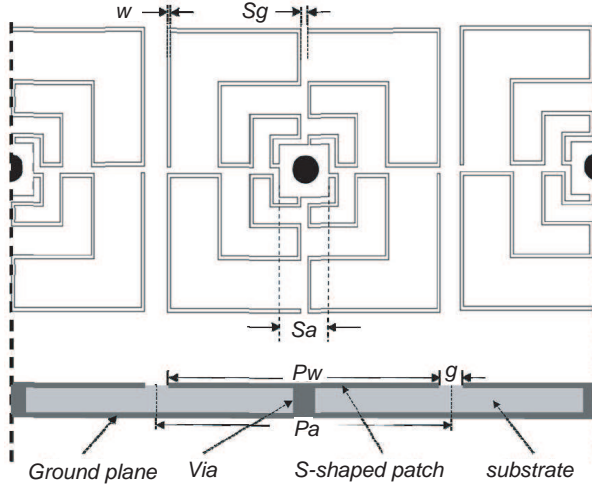


Figure 1. Geometry of the compact EBG cell.

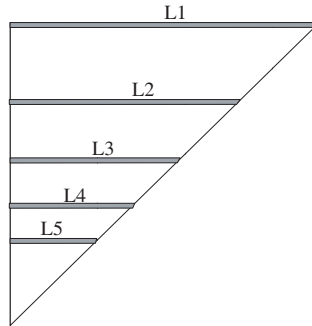


Figure 2. The log-periodic layout.

annular-slot antenna are selected as: $R_1 = 17.0$ mm, $R_2 = 12.0$ mm, the substrate size is $60 \text{ mm} \times 60 \text{ mm} \times 1.52 \text{ mm}$ and microstripline width W_{s1} is 3.0 mm, providing a 50Ω impedance and the length L_1 is 13.0 mm. To provide improved matching, a narrow line of width $W_{s2} = 1.0$ mm and length $L_2 = 12.0$ mm is connected to the 50Ω line and is coupled to the annular slot. This geometry was defined in a similar fashion as described in [19] to obtain a dualband behavior with both bands covered by the bandgaps of the EBG reflector.

In order to provide directional radiation properties, a reflector is used. A conventional metallic reflector is usually spaced at

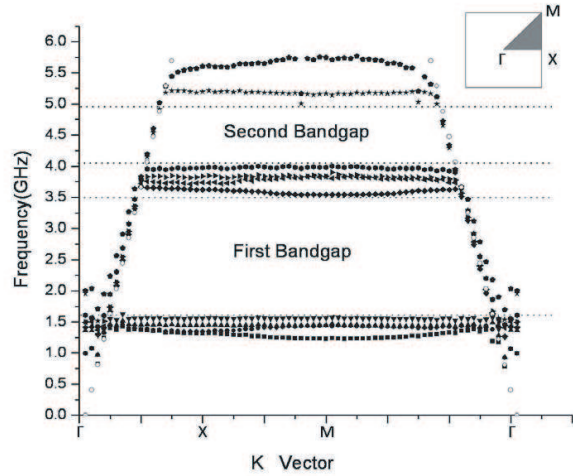


Figure 3. The dispersion curves for the proposed EBG structure.

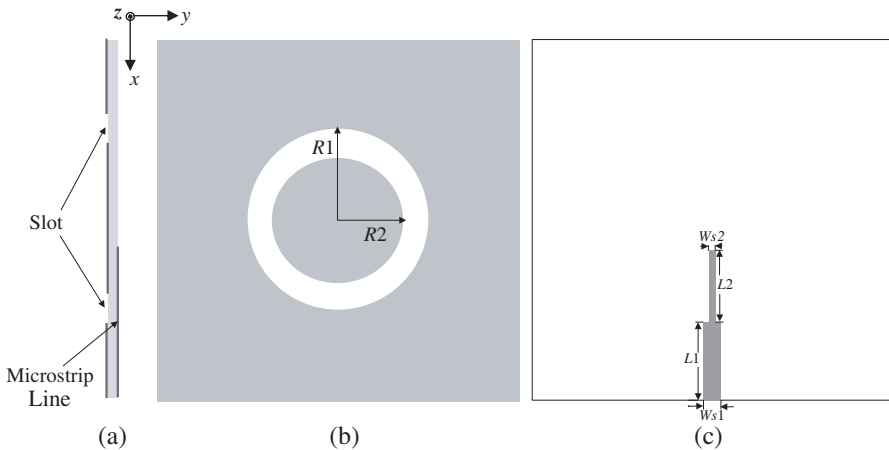


Figure 4. The geometry and coordinate system for the dualband slot antenna. (a) Substrate. (b) Slot in the groundplane. (c) Microstrip feedline.

approximately a quarter of a free space wavelength, but for dualband operation many trade-offs are necessary and performance is compromised. In this case a compact dualband EBG structure is proposed as the reflector which is shown in Figure 5(a). Both bandgaps for the EBG structure correspond to the annular slot antenna frequencies. A 5×5 array of EBG cells is utilized as a reflector and

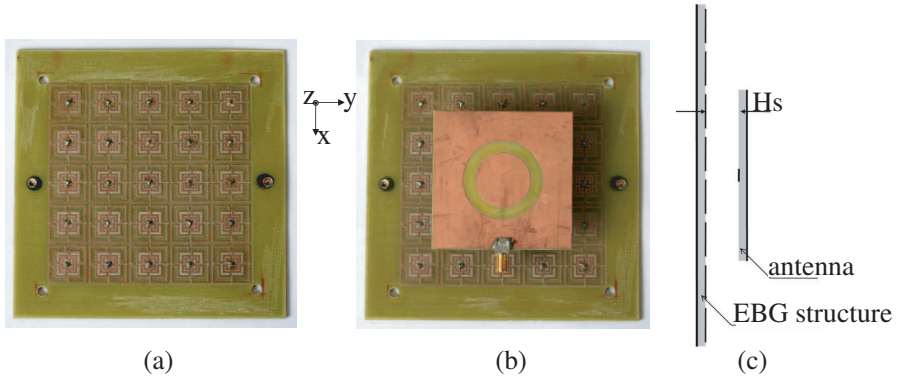


Figure 5. (a) Photo of compact 5 by 5 EBG cell reflector and (b) the proposed annular-slot antenna with EBG reflector; (c) drawing of the cross-section.

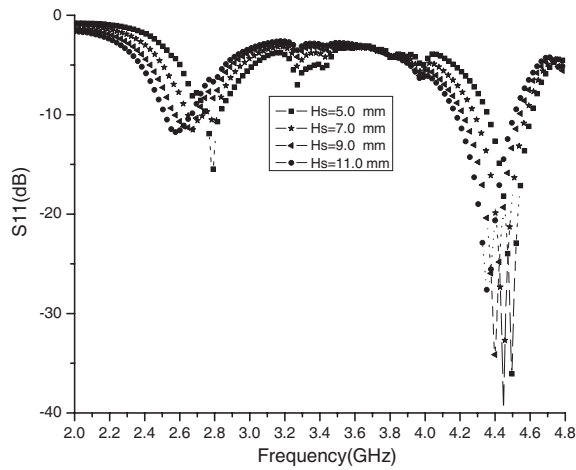


Figure 6. Simulated S_{11} for the proposed slot antenna for different spacings from EBG reflector.

combined with the slot antenna as shown in Figure 5(b). A foam layer is filled between the EBG structure and slot layer. This configuration can significantly reduce the spacing between the antenna and reflector plane, which is one-eighth of a wavelength at the lowest frequency, and provides reflector function for the two frequencies.

4. RESULTS AND DISCUSSION

Figure 6 shows the simulated S_{11} for the slot antenna/EBG reflector combination for different separation distances of $H_S = 5.0$ mm, 7.0 mm, 9.0 mm, and 11.0 mm. The plot shows an upward shift in frequency as the spacing is reduced. In this case, the spacing is selected to be 7.0 mm as it leads to a relatively wide bandwidth and good return

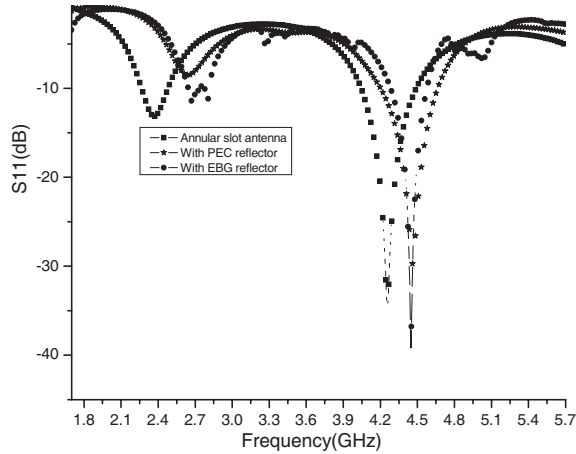


Figure 7. Comparison S_{11} of the slot antenna and the antenna with PEC and EBG reflectors.

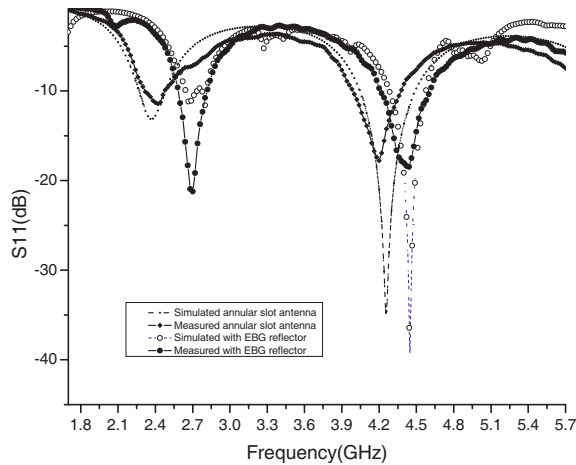


Figure 8. The simulated and measured S_{11} for the annular slot antenna with and without the EBG reflector.

loss for the both bands. For the annular-slot antenna, the 10 dB S_{11} bandwidths are approximately 185 MHz (2.274 GHz to 2.495 GHz) and 455 MHz (4.074 GHz to 4.529 GHz) for the two bands, as shown in Figure 7. The measured S_{11} for the antenna spaced 7.0 mm from the EBG reflector shows the bandwidths to be 167 MHz (2.647 GHz to 2.814 GHz) and 297 MHz (4.281 GHz to 4.578 GHz), respectively. Thus, the combination with EBG reflector causes a small upwards shift in matched frequency bands. When a conventional metallic plate reflector is used, an upward shift in matched frequency is also seen, but with very poor matching in the first band, while the bandwidth for the second band is 464 MHz (4.20 GHz to 4.664 GHz) as seen in Figure 7. Figure 8 shows the simulated and measured S_{11} for the slot antenna and the slot/EBG reflector combination. As seen in Figure 9, the gain of the proposed antenna is increased by 0.6 dB for each of the two bands compared to using the metal plate reflector under best match conditions. Even though the gain improvement obtained by using an EBG reflector instead of a conventional metallic plane is small, it should be noted that the EBG structure allows dual band behavior and a significant reduction of the spacing, H_s . In fact in the case of a metallic reflector a dual band behavior is not achievable as its distance from the antenna should be fixed at around $\lambda/4$. This would require a separation H_s of about 30 mm or 17 mm for the lowest and highest operating frequency, respectively.

Figure 10 and Figure 11 show the simulated and measured

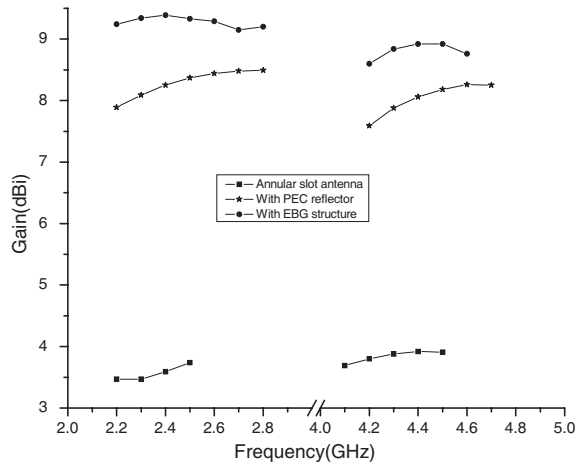


Figure 9. The measured gain for the standalone slot antenna and the antenna with PEC and EBG reflector.

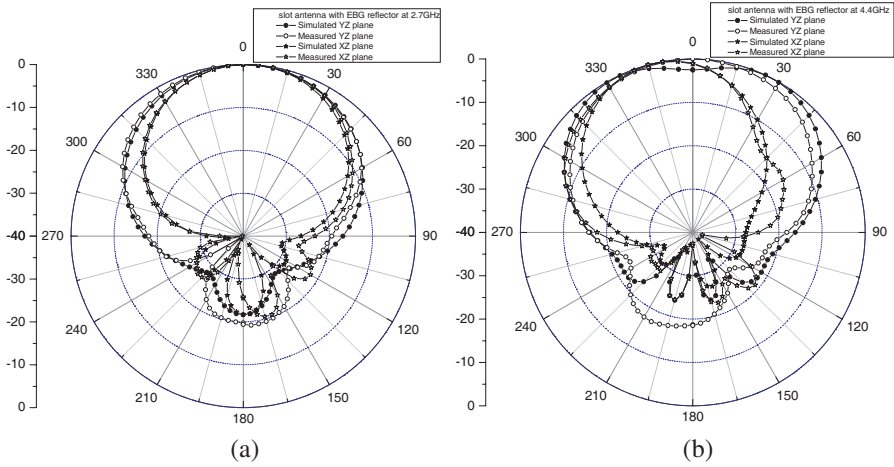


Figure 10. Simulated and measured normalized radiation antenna patterns for the antenna with EBG reflectors. (a) First band. (b) Second band.

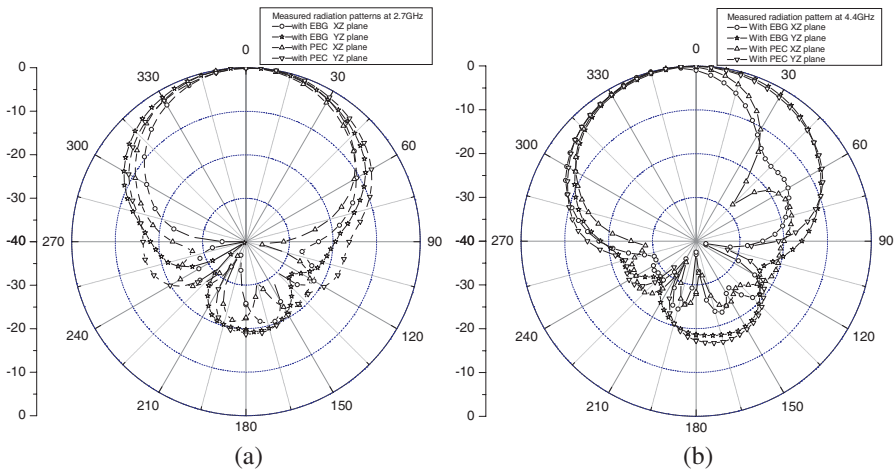


Figure 11. Measured normalized radiation patterns for the antenna with PEC and EBG reflectors. (a) First band. (b) Second band.

normalized radiation patterns in the XZ and YZ planes for the slot antenna with EBG reflector and compared to the to the slot with metallic plate reflector. The measured values are in agreement with numerical values. The slot antenna/EBG reflector combination achieves a directional performance with improved gain and lower profile, compared to a conventional reflector.

5. CONCLUSIONS

The novel compact EBG structure providing a dual-bandgap function is reported. In comparison with the conventional square patch high-impedance-surface, the proposed EBG structure is more compact. When used as a closely-spaced reflector for a dual band antenna, it provides greater gain compared to conventional reflectors over the two frequency bands.

REFERENCES

1. Lee, Y. C. and J. S. Sun, "Compact printed slot antennas for wireless dual and multi-band operations," *Progress In Electromagnetics Research*, PIER 88, 289–305, 2008.
2. Li, R. L., B. Pan, A. N. Traille, J. Papapolymerou, J. Laskar, and M. M. Tentzeris, "Development of a cavity-backed broadband circularly polarized slot/strip loop antenna with a simple feeding structure," *IEEE Transactions on Antennas and Propagation*, Vol. 56, No. 2, 312–318, 2008.
3. Song, Y. M., J. C. Modro, Z. P. Wu, and P. O’Riordan, "Miniature multiband and wideband 3-D slot loop antenna for mobile terminals," *IEEE Antennas and Wireless Propagation Letters*, Vol. 5, 148–151, 2006.
4. Irzinski, E. P., "The input admittance of a TEM excited annular slot antenna," *IEEE Transactions on Antennas and Propagation*, Vol. 23, No. 6, 829–835, 1975.
5. Bao, X. L. and M. J. Ammann, "Dual-frequency dual-sense circularly-polarized slot antenna fed by microstrip line," *IEEE Transactions on Antennas and Propagation*, Vol. 56, No. 3, 645–649, 2008.
6. Roy, R. and V. F. Fusco, "Dielectric-loaded cavity-backed slot radiator analysis," *IEE Proc.-Microwave, Antenna Propagation*, Vol. 47, No. 3, 195–198, 2000.
7. Qu, S. W., J. L. Li, Q. Xue, and C. H. Chan, "Novel unidirectional slot antenna with a vertical wall," *Progress In Electromagnetics Research*, PIER 84, 239–251, 2008.
8. Galejs, J. and T. W. Thompson, "Admittance of a cavity-backed annular slot antenna," *IEEE Transactions on Antennas and Propagation*, Vol. 10, No. 6, 671–678, 1962.
9. Elek, F., R. Abhari, and G. V. Eleftheriades, "A uni-directional ring-slot antenna achieved by using an electromagnetic band-

- gap surface," *IEEE Transactions on Antennas and Propagation*, Vol. 53, No. 1, 181–190, 2005.
10. Li, L., X. J. Dang, B. Li, and C. H. Liang, "Analysis and design of waveguide slot antenna array integrated with electromagnetic band-gap structures," *IEEE Antennas and Wireless Propagation Letters*, Vol. 5, 111–115, 2006.
 11. Gao, C., Z. N. Chen, Y. Y. Wang, N. Yang, and X. M. Qing, "Study and suppression of ripples in passbands of series/parallel loaded EBG filters," *IEEE Transactions on Microwave Theory and Techniques*, Vol. 54, No. 4, 519–1526, 2006.
 12. Liu, T. H., W. X. Zhang, M. Zhang, and K. F. Tsang, "Low profile spiral antenna with PBG substrate," *Electronics Letters*, Vol. 36, No. 9, 779–780, 2000.
 13. Sievenpiper, D., L. J. Zhnag, R. F. Broas, N. G. Alexopolous, and E. Yablonovitch, "High-impedance electromagnetic surface with a forbidden frequency band," *IEEE Transactions on Microwave Theory and Techniques*, Vol. 47, No. 11, 2059–2074, 1999.
 14. Baggen, R., M. M. Vazquez, J. Leiss, S. Holzwarth, L. S. Drioli, and P. Maagt, "Low profile GALILEO antenna using EBG technology," *IEEE Transactions on Antennas and Propagation*, Vol. 56, No. 3, 667–673, 2008.
 15. Rea, S. P., D. Linton, E. Orr, and J. McConnell, "Broadband high-impedance surface design for aircraft HIRF protection," *IEE Proc.-Microwave Antennas Propagation*, Vol. 153, No. 4, 307–313, 2006.
 16. Simovski, C. R. and A. A. Sochava, "High-impedance surface based on self-resonant grids. analytical modelling and numerical simulations," *Progress In Electromagnetics Research*, PIER 43, 239–256, 2003.
 17. Folayan, O. and R. J. Langley, "Wideband reduced size electromagnetic bandgap structure," *Electronics Letters*, Vol. 41, No. 20, 1099–1100, 2005.
 18. Bao, X. L., G. Ruvio, M. J. Ammann, and M. John, "A novel GPS patch antenna on a fractal Hi-impedance surface substrate," *IEEE Antennas and Wireless Propagation Letters*, Vol. 5, 323–326, 2006.
 19. Tehrani, H. and K. Chang, "Multifrequency operation of microstrip-fed slot-ring antennas on thin low-dielectric permittivity substrates," *IEEE Transactions on Antennas and Propagation*, Vol. 50, No. 9, 1299–1308, Sept. 2002.